The Out-of-band Response of the HRC on Chandra

M.V. Zombeck[1], M. Barbera[2], Y. Butt[1], J.J. Drake[1], F.R. Harnden, Jr.[1], S.S. Murray[1], B.J. Wargelin[1]

[1] Harvard-Smithsonian Center for Astrophysics, Cambridge MA (USA)
[2] Osservatorio Astronomico G.S. Vaiana, Palermo, Italy

ABSTRACT

We present models for the UV and visible light response of the HRC-I (High Resolution Camera-Imaging) and the HRC-S (High Resolution Camera-Spectroscopy) on the Chandra X-ray Observatory. Comparisons of predictions of the models with observed count rates will be given. The observed count rates are consistent with pre-launch predictions of the models. We also provide curves to predict the UV/Visible contamination for any star for which T_{eff}, V, and N_H are known.

1 INTRODUCTION

The High Resolution Camera (HRC)[1] on the Chandra X-ray Observatory[2] is a microchannel plate (MCP) instrument comprised of two detectors, one optimized for imaging (HRC-I) and one (HRC-S) serving as a readout for the Low Energy Transmission Grating (LETG). The HRC is a direct descendent of the Einstein and ROSAT High Resolution Imagers (HRIs). In order to increase the quantum efficiency for X-ray detection the front microchannel plate of each of the HRC detectors is coated with CsI. This results in extending the response of the microchannel plate well into the UV and visible, and a blocking filter was placed in front of each detector's MCP assembly in order to eliminate contamination from sources with significant UV flux. The ROSAT HRI's front microchannel plate was also coated with CsI and suffered from sensitivity to bright stars. This has been attributed[3,4] to enhanced transmission of the aluminized Lexan blocking filter longward of 2000 Å. As a result of the ROSAT experience, the HRC team investigated a number of materials that would provide better UV blocking and eliminated coating both sides of the filter with aluminum, which leads to an enhancement of the filter's transmission due to interference effects. Aluminized polyimide was found to meet our blocking requirements. Figure 1 illustrates the design of the blocking filters[5] for the two HRC detectors. The HRC-I filter consists of a single homogeneous filter, whereas the HRC-S filter comprises three segments, the outer two being identical. Within each segment there is a single thickness of polyimide with two different thicknesses of aluminum. The preflight predicted UV response of the HRC was based on a combination of transmission measurements of sample blocking filters, literature values for the quantum efficiency of the CsI coating, and measurements of the flight detector's quantum efficiency at only three wavelengths: 1470, 1850, and 4500 Å.

2 OUT-OF-BAND EFFECTIVE AREA MODELS

Effective area models for the individual filter components were obtained by multiplying the quantum efficiency of the MCP by the transmissions of the blocking filters and the CXC HRMA (High Resolutiom Mirror Assembly) geometric collecting area. The quantum efficiency of the CsI coated microchannel plates is only known at one wavelength (5500 Å) beyond 2537 Å (HgI from mercury vapor lamp). We constructed two plausible models for the quantum efficiency beyond 2537 Å by interpolating between these two data points with either a logarithmic interpolation (high QE model) or an exponential function, which fits the data shortward of 2537 Å, combined with a constant value equal to the measured quantum efficiency at 5500 Å (low QE model). We arbitrarily reduce the quantum efficiency beyond 6000 Å to zero for the latter model. See Ref. 3 for a more detailed discussion of the models. The sparse QE measurements of the flight detectors in the laboratory favor the low QE model and we will employ it below. The count rate predictions for the two different models are only significant for stars with effective temperatures below 6500 K and differ by less than a factor of two (for HRC-S) to eight (for HRC-I). Figures 2 and 3 show the derived effective area models.

3 PREDICTED UV/VISIBLE COUNT RATES FOR STARS

Following Ref. 4, we have derived a family of curves for predicting the UV/Visible count rates for stars with effective temperatures in the range from 3000 to 40000 K. The dereddened spectra of a set of sample stars (see Table 1) covering this range, were normalized to V=0, attenuated by various hydrogen column densities, and folded with the effective area models. The dereddened visible spectra (3500 - 7400 Å) were derived from calibrated spectra of parent spectral type stars[6]. The IUE spectrum of the sample stars were dereddened by using Seaton's[7] extinction function. Figure 4 shows the dereddened spectra of the sample stars and the effect of absorption by an interstellar hydrogen column density $N_H = 2 \times 10^{21}$ cm^{-2}. Figures 5 and 6 show the predicted HRC count rates as a function of effective temperature T_{eff} and hydrogen column density for a dereddened visual magnitude of 0. To find the UV/Visible count rate for a star of apparent visual magnitude V, multiply the value obtained for a specific T_{eff} and N_H by $10^{-(V-3.2E(B-V))/2.5}$, where E(B-V) is the star's color excess[8].

4 IN-FLIGHT RESULTS

During the calibration phase of the Chandra X-ray Observatory, Vega (A0V, V=0.03) was observed by the HRC-I and HRC-S. The UV/Visible response was tested by observing Vega at the nominal aim point on both the HRC-I and HRC-S, as well as two off-axis locations on the HRC-S with higher filter transmissions. The observed and predicted rates are shown in Table 2. Given the crudeness of the model, the agreement (predictions factors of 2-4 higher) between predicted and observed rates is remarkable. We note that the ROSAT HRI observation of Vega yielded a count rate of 0.1 ct s^{-1}. Since the geometric collecting area of ROSAT was almost identical to that of Chandra we have reduced the UV/Visible light contamination from Vega by a factor of at least 75 for HRC-I by using the polyimide blocking filter instead of Lexan. We plan further in-flight observations to improve the models and will be making more laboratory measurements to determine the quantum efficiency of CsI coatings in the UV and visible region of the spectrum.

5 ACKNOWLEDGEMENTS

We acknowledge partial support by NASA contract NAS8-38248 and by the Agenzia Spaziale Italiana, and the Ministero della Ricerca Scientifica e Tecnologica. The authors acknowledge Gary Meehan for useful suggestions and comments.

6 REFERENCES

1. Murray, S.S., et al., SPIE, 4012, 68, 2000.
2. Weisskopf, M.C., et al., SPIE 4012, 2, 2000.
3. Zombeck, M. V., et al., Ap. J. Lett., 487, L69, 1997.
4. Barbera, M., et al., Ap. J., 2000.
5. Meehan, et al., SPIE, 3114, 11, 1997.
6. Jacoby, G.H., et al., Ap. J. Suppl., 56, 257, 1984.
7. Seaton, M.J., MNRAS, 187, 73P, 1979.
8. Mihalas, D. and Binney, J., Galactic Astronomy, W.H. Freman and Company, 1981.

7 Tables and Figures

Table 1: List of sample stars covering the T_{eff} range 3000-40000 K.

Star	HR	HD	Sp	V [mag]	T_{eff} [K]	$\log(N_H)$ [cm^{-2}]	IUE Spectra
	8023	199579	O6V	5.96	40000	21.04	SWP09429, LWP03855
ν ORI	1855	36512	B0V	4.62	30000	20.35	SWP08164, LWR07097
λ LIB	5902	142096	B2.5V	5.03	20000	21.09	SWP42326, LWR10778
35 ERI	1244	25340	B5V	5.28	15000	20.06	SWP49909, LWP27312
Vega	7001	172167	A0V	0.03	9500	18.00	SWP27024, LWP07904
70 TAU	1391	27991	F7V	6.46	6500	19.00	SWP09853, LWR06639
V911 TAU		28099	G6V	8.12	5500	19.00	SWP09873, LWP02601
Betelgeuse	2061	39801	M1I	0.50	3200	19.80	SWP37517, LWP19982

Table 2: Comparison of observed count rates for Vega with model predictions. The UV/Visible response was tested by observing Vega at the nominal aim point on both the HRC-I and HRC-S, as well as two off-axis locations on the HRC-S with higher filter transmissions.

Detector	UVIS Segment*	Obs. Count Rate (s^{-1})	Pred. Count Rate (s^{-1})
HRC-I	HRC-I	$< 1.4 \times 10^{-3}$	7.4×10^{-4}
HRC-S	Seg0 thick Al	0.17 ± 0.01	0.9
HRC-S	Seg0 thin Al	240 ± 0.4	391
HRC-S	Seg+1 thin Al	475 ± 0.7	1960

* See Figure 1 for thicknesses.

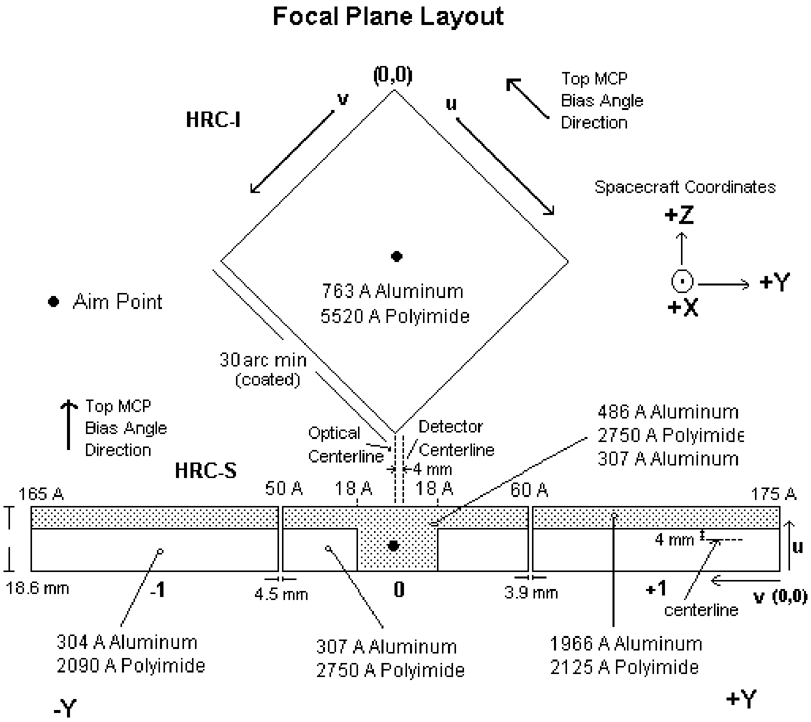

Figure 1: Configuration of the UV/Ion shields (blocking filters) of the HRC-I and HRC-S detectors. The UV/Visible response was tested by observing Vega at the nominal aim point on both the HRC-I and HRC-S, as well as two off-axis locations on the HRC-S with higher filter transmissions.

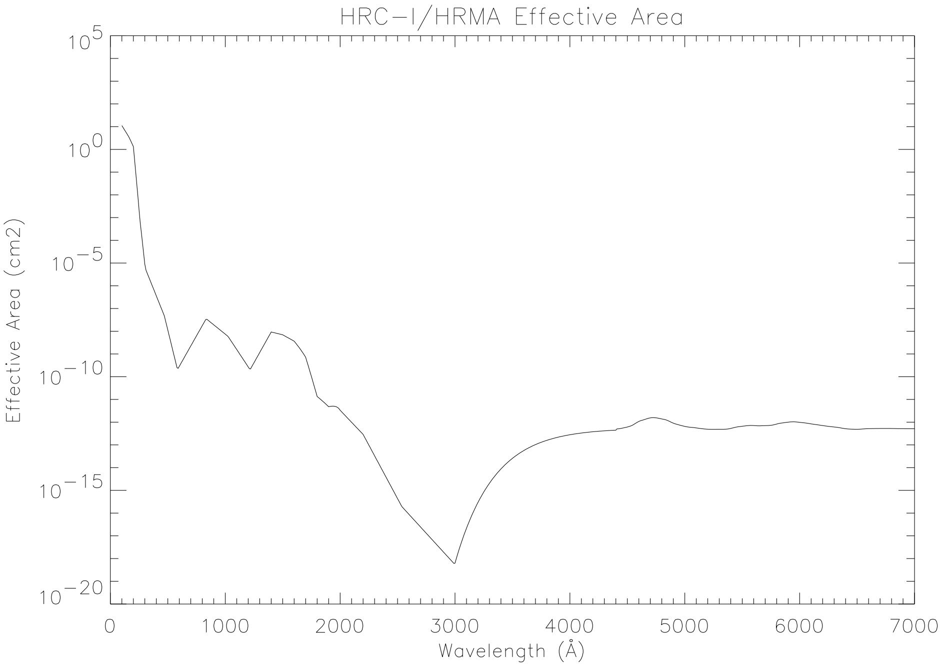

Figure 2: HRC-I/HRMA effective area. A wavelength independent area of 1100 cm^2 was assumed for the HRMA

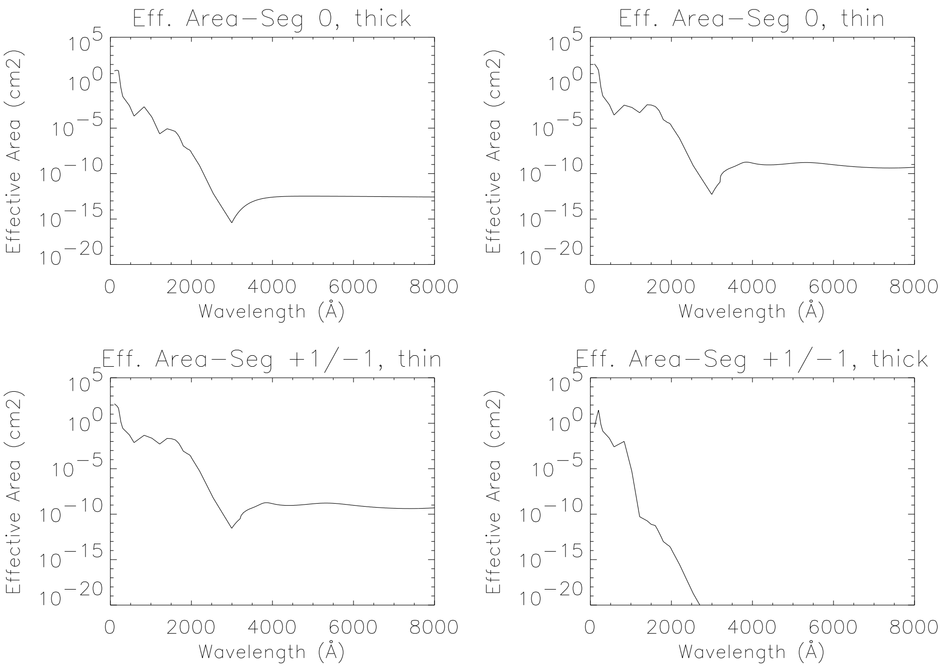

Figure 3: HRC-S/HRMA effective areas for the various UV/Ion shield segments. A wavelength independent area of 1100 cm^2 was assumed for the HRMA.

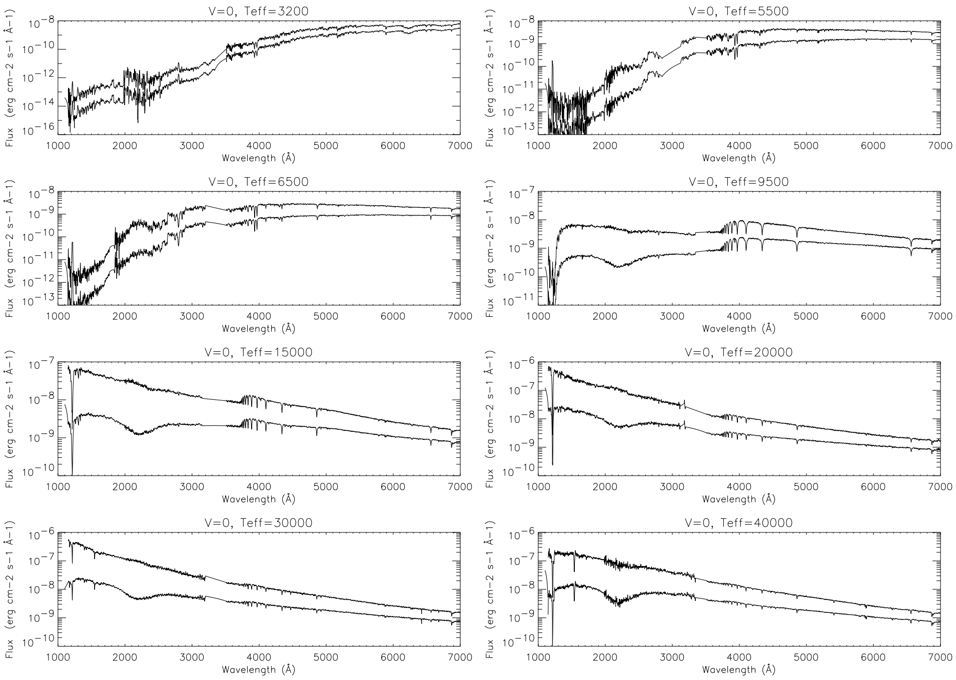

Figure 4: UV/Visible spectra of the sample stars (dereddened and normalized to V=0) of Table 1. The lower curve for each panel is the same spectrum attenuated by an N_H of 2×10^{21} cm^{-2}.

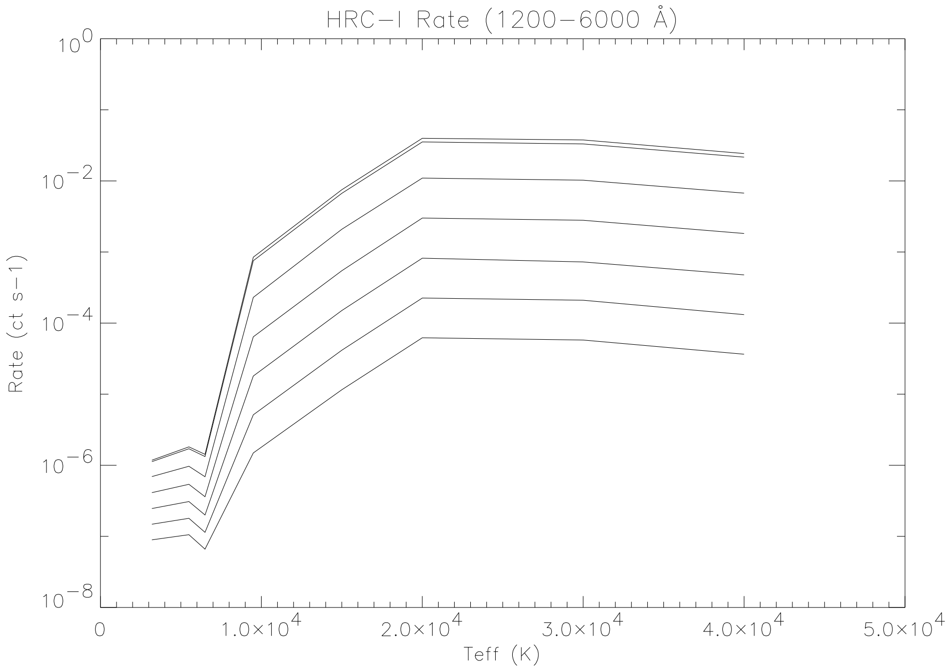

Figure 5: Predicted HRC-I rates for stars normalized to V=0 (dereddened) as a function of T_{eff} and for $N_H =$ $1{\times}10^{19}$, 1×10^{20}, 1×10^{21}, 2×10^{21}, 3×10^{21}, 4×10^{21}, and 5×10^{21} cm^{-2} (top to bottom).

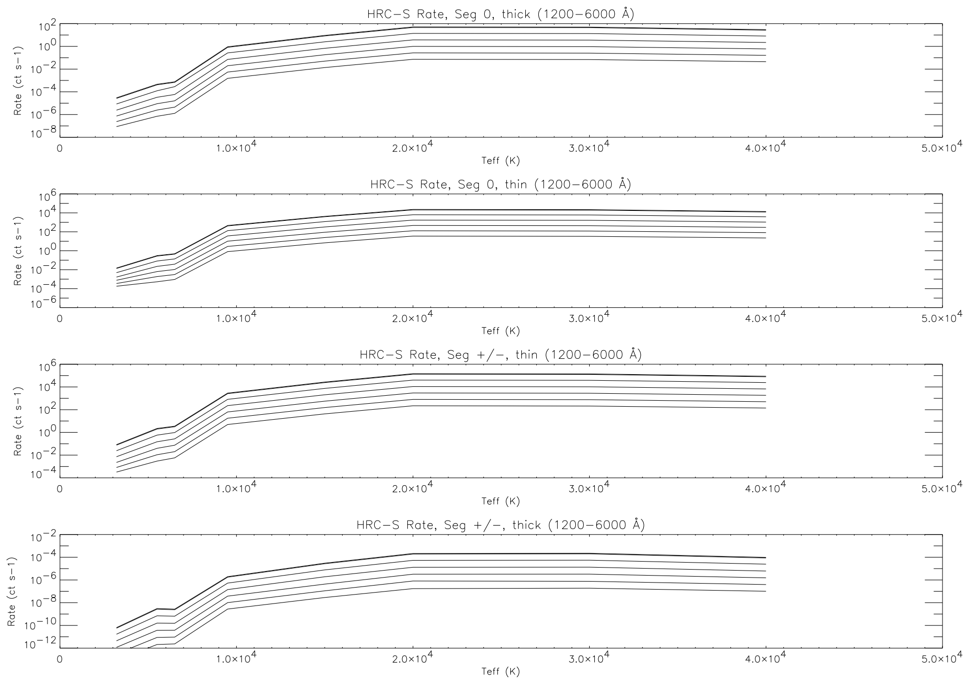

Figure 6: HRC-S rates for the various UV/Ion shield segments for stars normalized to V=0 (dereddened) as a function of T_{eff} and for $N_H = 1 \times 10^{19}$, 1×10^{20}, 1×10^{21}, 2×10^{21}, 3×10^{21}, 4×10^{21}, and 5×10^{21} cm^{-2} (top to bottom).